NACA TN 1923

NATIONAL ADVISORY COMMITTEE FOR AERONAUTICS

TECHNICAL NOTE 1923

BOUNDARY-LAYER AND STALLING CHARACTERISTICS OF THE NACA 64A006 AIRFOIL SECTION

By George B. McCullough and Donald E. Gault

Ames Aeronautical Laboratory
Moffett Field, Calif.

CASE FILE COPY

Washington
August 1949

NATIONAL ADVISORY COMMITTEE FOR AERONAUTICS

TECHNICAL NOTE 1923

BOUNDARY-LAYER AND STALLING CHARACTERISTICS OF THE NACA 64A006 AIRFOIL SECTION

By George B. McCullough and Donald E. Gault

SUMMARY

The boundary-layer and stalling characteristics of an NACA 64A006 airfoil section were investigated experimentally at a Reynolds number of 5,800,000. The data presented include measurements of lift, drag, and pitching moment, chordwise distribution of pressure, visual studies of the boundary-layer flow, and surveys of the static-pressure and velocity distribution within the boundary layer.

At 5° angle of attack (c_l = 0.56), an extensive region of separated flow, covering approximately the forward 0.08 chord, appeared abruptly accompanied by discontinuities in the section lift, drag, and moment characteristics. With increasing angle of attack, the chordwise extent of the region of separated flow progressively increased until the flow over the entire upper surface was separated at the angle of attack for maximum lift (α_o = 9°, c_l = 0.89). In consequence of this gradual expansion of separated flow, the peak of the lift curve was rounded. There was no abrupt loss of lift after the attainment of maximum lift.

INTRODUCTION

As part of a general investigation of the stalling properties of wings, a detailed study of thin wing sections has been undertaken. The purpose of the study was to gain a better understanding of the mechanism of stalling, particularly for wing sections subject to separation of flow from the leading edge. Knowledge of this type of stall gains importance in view of the fact that airfoil sections suitable for high-speed application usually stall from the leading edge at relatively low values of lift coefficient. Further, the sequence of the stall over a wing may produce such pronounced stability and control difficulties as to limit seriously the low-speed operation of the airplane. It is hoped that knowledge of the mechanism of the stall may lead to methods of alleviating its more undesirable effects.

An investigation of the stalling and boundary-layer characteristics of the NACA 63-009 airfoil section has been completed and is reported in reference 1. The present report presents the results of a similar study for an NACA 64A006 airfoil section. The data were obtained in the Ames 7- by 10-foot wind tunnel No. 1 and include measurements of lift, drag, and pitching-moment, chordwise distribution of pressure, visual studies of the boundary-layer flow, and extensive surveys of the static and total pressure within the boundary layer.

SYMBOLS

The symbols used in this report are defined as follows:

c wing chord, feet

c_d section drag coefficient $(D/q_o c)$

c_l section lift coefficient $(L/q_o c)$

c_m section pitching-moment coefficient referred to the quarter chord $(M/q_o c^2)$

D drag per unit span, pounds

h local total pressure within boundary layer, pounds per square foot

H_o free-stream total pressure, pounds per square foot

L lift per unit span, pounds

M pitching moment per unit span, pound-feet

p local static pressure within boundary layer, pounds per square foot

p_l local static pressure at outer edge of boundary layer, pounds per square foot

q_o free-stream dynamic pressure $(\frac{1}{2}\rho_o U_o^2)$, pounds per square foot

S pressure coefficient $\left(\frac{H_o - p}{q_o}\right)$

u local velocity inside boundary layer, feet per second

U local velocity outside boundary layer, feet per second

U_o free-stream velocity, feet per second

x distance from airfoil leading edge measured parallel to chord line, feet

y distance above airfoil measured normal to surface, feet

α_o geometric angle of attack, degrees

ρ_o free-stream mass density, slugs per cubic foot

APPARATUS AND TESTS

Apparatus

Model.- The model was constructed of laminated mahogany laid over a steel spar. Coordinates of the NACA 64A006 airfoil section are given in reference 2. The chord was 5 feet and the span 7 feet, extending from the floor to the ceiling of the wind tunnel. (See fig. 1.) Circular plates, 6 feet in diameter, attached to the ends of the model formed part of the tunnel walls. Flush-type pressure orifices were built into the midspan section of the model.

Boundary-layer rakes.- Surveys of the flow within the boundary layer were made with pressure-measuring rakes made of small-diameter tubing attached to the surface of the model. Static- and total-pressure tubes were made into separate rakes, usually matched as to size and tube spacing. A pair of 10-inch rakes may be seen in figure 1. The middle rake visible in the photograph was used to obtain the total-pressure distribution close to the surface. Near the leading edge where the boundary layer was thin, smaller rakes were used. The smallest rakes were made of hypodermic tubing 0.015 inch in diameter. The heights of the tubes above the surface of the model were measured to the nearest 0.01 inch with a steel scale and magnifying glass. For heights less than 0.10 inch a micrometer microscope was used.

Limitations of boundary-layer rakes.- The boundary-layer measurements made during the course of the present investigation are not strictly quantitative because of certain inadequacies and limitations of small pressure-measuring rakes as boundary-layer measuring devices. Although these shortcomings are present to a certain extent under any circumstances, they become accentuated when attempting to measure the boundary-layer flow of thin airfoils subject to separation from the leading edge. An enumeration of possible sources of error in the boundary-layer measurements of the present investigation is given in the following paragraphs.

The presence of the rakes, which were relatively large in order to bracket the large outward displacement of flow which accompanied separation, and the associated leads undoubtedly had an appreciable effect on the flow around the airfoil. Moreover, the fact that the detached boundary layer was thin in comparision with the underlying region of relatively stagnant air meant that only a few of the rake tubes were within the detached boundary layer itself, thus yielding only a few points to define its velocity profile.

A further difficulty arose from the inclination of the flow to the surface of the model. When the flow became sufficiently oblique to the axes of the total- or static-pressure tubes of the rakes, the tubes no longer indicated the true total or static pressure of the flow. For the present investigation this difficulty was overcome. partially at least, by bending the total-pressure tubes in the direction of the flow until the tubes outside of the boundary layer recovered free-stream total pressure. The tubes of the static-pressure rake were then bent parallel with those of the total-pressure rake.

Another possible source of error was concerned with the determination of the height of the separated region (the point above the surface where the total and static pressures were equal), and resulted from large relatively low-frequency fluctuations of velocity associated with the separated boundary layer.[1] In such a flow regime, a total-pressure tube indicates a greater pressure than the true mean total pressure. This characteristic of total-pressure tubes necessitated a more or less arbitrary fairing of the total-pressure data.

Tests

Force measurements were made with the wind-tunnel balance system prior to the boundary-layer surveys. All pressures were recorded by photographing liquid-in-glass manometers.

Visual indications of the boundary-layer flow were obtained by observing the action of short tufts of thread glued to the surface of the model, and also by the liquid-film method described in reference 1.

Unless otherwise mentioned, all tests were made at a dynamic pressure of 40 pounds per square foot which corresponds to a Mach number of 0.167 and a Reynolds number of 5,800,000.

---

[1]The existence of these fluctuations was verified by placing a 1/4-inch-diameter static-pressure tube within the separated region and connecting the tube to a recording pressure cell. Fluctuations in static pressure averaging about 20 cycles per second were recorded.

RESULTS AND DISCUSSION

Force and Moment Characteristics

The lift, drag, and pitching-moment characteristics as determined from the wind-tunnel balance system and from graphical integration of the chordwise pressure distribution are shown in figure 2. Both the normal and the chordwise components of the pressure distribution were considered in the computation of the force and moment characteristics. Corrections for jet boundary effects[2] have not been applied because free-air conditions would not correspond to the conditions under which the boundary-layer measurements were obtained. Values of the section lift coefficient mentioned in the following discussion and in the figures are those computed from the pressure distributions. They are believed to be more representative of conditions at the midspan section of the model where the boundary-layer surveys were made.

The variation of lift with angle of attack was characterized by a discontinuity or failure of the lift to increase linearly near 5° angle of attack ($c_l = 0.53$). A limited test was made at a Reynolds number of 8,100,000. The appearance of the discontinuity was delayed to an angle of attack $1/2^\circ$ higher. As will be shown later, the discontinuity in lift was associated with the formation of an appreciable region of separated flow near the leading edge of the model. The separated region increased in chordwise extent as the angle of attack was increased.

For angles of attack greater than 5°, the slope of the lift curve was reduced and the peak of the curve was rounded with no sudden loss of lift at the stall. The maximum section lift coefficient was 0.89 and occurred at an angle of attack of 9°. (It should be mentioned that successive force measurements showed considerable scatter in the vicinity of maximum lift. This is thought to have been caused by the buffeting which accompanied the stall of the model and its effect on the mechanical wind-tunnel balance system.)

Associated with the jog in the lift curve there was an abrupt increase in the drag of the model. The reason for the discrepancy between the two drag curves is that the drag as measured by the balance system included the tare drag of the circular plates on the ends of the model and, of course, the skin-friction drag. The minimum section profile-drag coefficient as determined by the wake-survey method was 0.0039. The abrupt increase of drag at 5° angle of attack was primarily caused by a sudden increase in pressure drag.

---

[2]The method usually employed for correcting the data to free-air conditions is described in reference 3.

A small positive shift of the section pitching-moment coefficient accompanied the discontinuity in lift, followed by a progressively increasing negative trend for values of the lift coefficient greater than 0.65.

Pressure Distribution

The chordwise distribution of the pressure coefficient S over the surface of the model is shown in figure 3. In order to depict the pressure peaks more clearly, the pressure distribution over the first 5-percent chord is plotted to an expanded scale in figure 4. The values of the pressure coefficient are the measured uncorrected values.

The peak pressure coefficients over the leading edge attained a maximum value at an angle of attack of about 4.5° ($c_l = 0.53$). A small region of constant pressure, indicative of a narrow band of laminar separation similar to that found on a 9-percent-thick section (reference 1), is discernible in the pressure distributions for 3°, 4°, and 4.5° angle of attack. For angles of attack of 5° and greater a different type of flow separation occurred, and the pressure peak progressively collapsed accompanied by the appearance of a greatly enlarged region of approximately constant pressure.

The small flow disturbance indicated for angles of attack from 3° to 4.5° caused no appreciable effect on the measured values of lift, drag, or pitching moment, but the partial collapse of the pressure peak at 5° angle of attack did produce an abrupt change in these characteristics. As the angle of attack was further increased the region of constant pressure expanded rearwardly. The ensuing change in chordwise loading was reflected in the strong negative trend of the pitching moment for angles of attack of 7° and greater. At maximum lift the region of approximately constant pressure covered the forward 40 percent of the upper surface.

The manner in which the pressures over the model varied with angle of attack is shown in figure 5. The experimentally measured values of the pressure coefficient for the angle-of-attack range between 0° and 4.5° agreed excellently with those computed from the theoretical chordwise velocity distribution given in reference 2. Between 4.5° and 5° the pressures at most chordwise stations varied discontinuously. For angles of attack of 5° or greater, the pressure coefficients over the rearmost 20 to 30 percent of the upper surface (fig. 5(a)) increased continuously up to 11° angle of attack, at least. Farther forward, the pressure coefficient tended to remain constant or to decrease slightly before beginning to increase rapidly with increasing angle of attack (except forward of 0.01 chord, where the pressure coefficient decreased constantly after the collapse of the pressure peak (cf., fig. 4)). At each chordwise station the rapid increase in pressure coefficient with angle of attack began before the region of separated flow (the boundary of which is indicated by the

shaded area in fig. 5(a)) reached the station, and continued to increase after the region extended downstream of the station. Because of the increasing extent of the region of approximately constant pressure, the pressure coefficients in figure 5(a) tend to decrease along a common path with increasing angle of attack.

The pressures at the lower surface stations (fig. 5(b)) tended to remain more nearly constant for angles of attack greater than 6°. The stagnation point remained fixed at 0.005 chord for angles of attack from 4.5° to 11° despite an increase in section lift coefficient from 0.53 to 0.89.

The complete stall of the model was the result of a gradual readjustment of the pressure distribution. This is in contrast to the abrupt readjustment of pressure distribution experienced by the NACA 63-009 airfoil section which produced a sharp peak on the lift curve (reference 1). There was, however, a similarity in the shape of the pressure distribution of the 9-percent-thick airfoil after the stall to that of the 6-percent-thick airfoil immediately prior to the stall.

Boundary-Layer Characteristics

Visual studies.- Visual observation of the action of tufts of thread glued to the surface of the model indicated smooth flow for angles of attack up to 4.5° (c_l = 0.53). At this point there were indications of intermittent separation of flow near the leading edge. As the angle of attack was further increased, the leading-edge separation persisted and gradually spread downstream. The tufts downstream of the separated area indicated very rough flow. As the extent of the area of separated flow increased, a definite reversed flow appeared in the middle of the area. At an angle of attack of about 8° the flow over the entire upper surface of the model appeared to be separated.

Attempts to ascertain the character of the boundary-layer flow by spraying the model with a thin film of a mixture of alcohol, glycerin, and Aerosol were not very successful because the patterns formed by the liquid film were indefinite, particularly at the downstream boundary of the region of separated flow. There was, however, an irregular spanwise ridge of liquid which formed initially at 3° angle of attack, suggestive of a narrow band or "bubble" of separated flow. The chordwise location of this ridge agreed well with the flat spot in the detailed pressure distribution of figure 4. At larger angles of attack the liquid film gave a good demonstration of the reversed flow in the separated region by the forward movement of detached flecks of froth.

Velocity profiles.- Boundary-layer velocity profiles were computed from the measured static and total pressures according to the relationship

$$\frac{u}{U} = \sqrt{\frac{h-p}{H_o - p_l}}$$

The height of the outer edge of the boundary layer was determined by the distance above the surface to the point where the total pressure attained free-stream total pressure. In the case of separated boundary layers, the height of the layer underlying the separated flow was taken as the point where the indicated total pressure equalled or most closely approached the static pressure.

Boundary-layer profiles measured at various chordwise stations for three angles of attack are shown in figure 6. The profiles in figure 6(a) were obtained at an angle of attack of 4° ($c_l = 0.47$), and show the normal growth of the boundary layer as it progressed downstream along the chord. The localized region of separated flow evidenced by the liquid film at an angle of attack of 4° was not found by direct boundary-layer measurements. It is believed that the diameter of the survey tubes was so great in comparison with the thickness of the region that the tubes recovered the pressure corresponding to the outer separated flow, and therefore failed to furnish an indication of the presence of the bubble. Boundary-layer profiles measured for an angle of attack of 5° ($c_l = 0.56$) are shown in figure 6(b). Note that the scale for the distance above the surface y/c has been compressed by a factor of 10 because of the pronounced thickening of the boundary layer. The profiles measured at 2.5- and 5.0-percent chord were separated from the surface, but at 10-percent chord the boundary layer had reattached with an unusual shape of the velocity profile. Farther downstream, however, the boundary layer assumed the velocity distribution usually associated with a turbulent boundary layer.

In figure 6(c) are the velocity profiles measured for an angle of attack of 7° ($c_l = 0.75$). These profiles were separated at 30-percent chord but reattached at approximately 35-percent chord. Profiles are shown to 60-percent chord only. Farther downstream the turbulent boundary layer was thicker than the tallest rakes used in this investigation.

Many more boundary-layer profiles than those presented in figure 6 were measured, but in general appearance they were similar to those shown. A summary of some of these data giving the height and extent of the layer underlying the separated flow for several angles of attack is shown in figure 7. The large region of separation was first discernible by boundary-layer velocity surveys at an angle of attack of 5° at which point it covered approximately the first 8 percent of the chord. The thickness of the underlying layer was about 0.3 inch ($y/c = 0.005$). With increasing angle of attack, the separated region grew in both thickness and chordwise extent until it covered the entire upper surface of the model at the angle of attack corresponding approximately to maximum lift ($\alpha_o = 9^\circ$, $c_l = 0.89$). The maximum thickness of the underlying layer for boundary-layer flow which

reattached to the surface was about 2.1 inches (y/c = 0.035) and occurred at about 25-percent chord.

Static-pressure variation.- The variations of the static pressure above the surface of the model for angles of attack of 4°, 5°, and 7° are shown in figure 8. The heights of the layer underlying the separated flow and the total thickness to the outer edge of the boundary layer are also indicated. The static pressures are presented in the same coefficient form as the chordwise pressure distributions of figures 3 and 4.

For an angle of attack of 4° (fig. 8(a)), the static pressure above the surface of the model was relatively constant except in the vicinity of the leading edge. The static orifices in the surface of the model consistently indicated lower pressures than the tubes of the static rake. The reason for this is not understood, but it is believed to be caused in part, at least, by the presence of the rakes on the surface of the model. (The surface pressure measurements and the boundary-layer surveys were made independently.)

At the higher angles of attack (figs. 8(b) and 8(c)), a pronounced variation in static pressure appeared; the static-pressure coefficient increased with increasing distance above the surface, then decreased. This variation was most pronounced in the vicinity of the region of separated flow and tended to disappear after the boundary layer reattached and passed downstream. As was mentioned in reference 1, the variation of static pressure near the leading edge was strongly suggestive of a vortex with its core at the point of minimum static pressure. The existence of a vortex would account for the reversed flow observed on the surface of the model. A comparison of these boundary-layer characteristics with those obtained for a 9-percent-thick section (reference 1) reveals a similarity of the flow over the 6-percent-thick section prior to the attainment of maximum lift to that of the 9-percent-thick section after the attainment of maximum lift.

SUMMARY OF RESULTS

The investigation of the stalling and boundary-layer characteristics of an NACA 64A006 airfoil section showed the following:

At 3° angle cf attack ($c_l = 0.35$), the pressure distribution and liquid-film studies indicated the presence of a small bubble of separated flow on the upper surface near 0.5-percent chord (cf., reference 1). At 5° angle of attack ($c_l = 0.56$), an abrupt change in the character of the flow took place and a greatly enlarged region of separated flow appeared. The boundary-layer flow detached from the upper surface near the leading edge then reattached at about 8-percent chord, leaving beneath it an underlying layer of relatively dead air. This abrupt change in flow was accompanied by a discontinuity in lift and an increase in drag. For greater

angles of attack, the region underlying the separated flow progressively thickened and extended toward the trailing edge until, at maximum lift ($\alpha_o = 9^\circ$, $c_l = 0.89$), the flow was separated over the entire upper surface of the model.

The cause of the discontinuity in lift at 5° angle of attack was a partial collapse of the peak pressures near the leading edge accompanied by the formation of a region of approximately constant pressure. This redistribution of pressure also caused the increase in drag and a small positive shift of the pitching moment. With increasing angle of attack the region of approximately constant pressure expanded rearwardly, thereby producing an increasingly negative pitching moment. Beyond maximum lift there was no abrupt redistribution of pressure and, consequently, no sudden loss of lift.

Ames Aeronautical Laboratory,
National Advisory Committee for Aeronautics,
Moffett Field, Calif., June 6, 1949.

REFERENCES

1. Gault, Donald E.: Boundary-Layer and Stalling Characteristics of the NACA 63-009 Airfoil Section. NACA TN 1894, 1949.

2. Loftin, Laurence K.,Jr.: Theoretical and Experimental Data for a Number of NACA 6A-Series Airfoil Sections. NACA TN 1368, 1947.

3. Allen, H. Julian, and Vincenti, Walter G.: Wall Interference in a Two-Dimensional-Flow Wind Tunnel, with Consideration of the Effect of Compressibility. NACA Rep. 782, 1944.

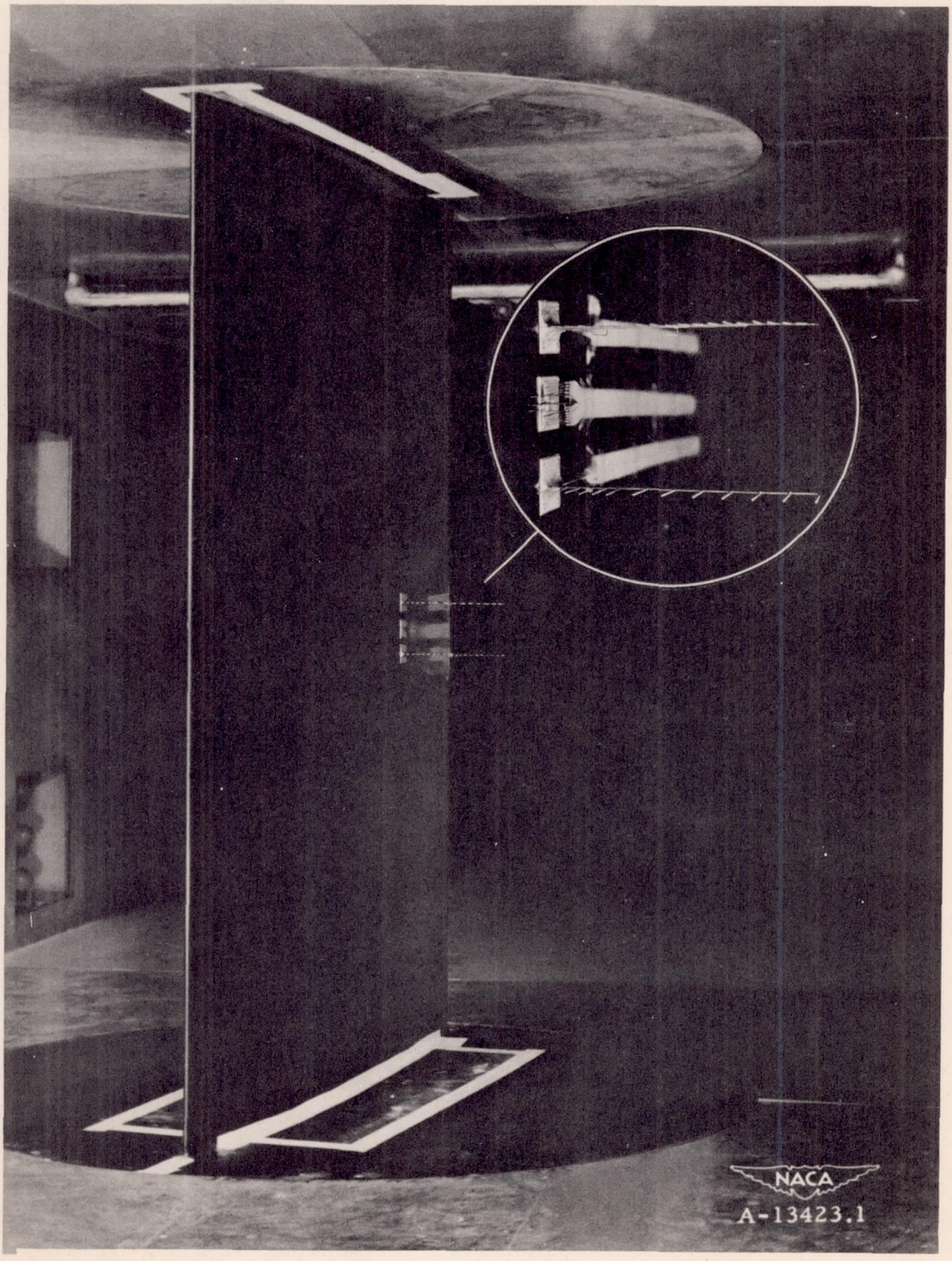

Figure 1.– The NACA 64A006 airfoil model installed in the wind tunnel.

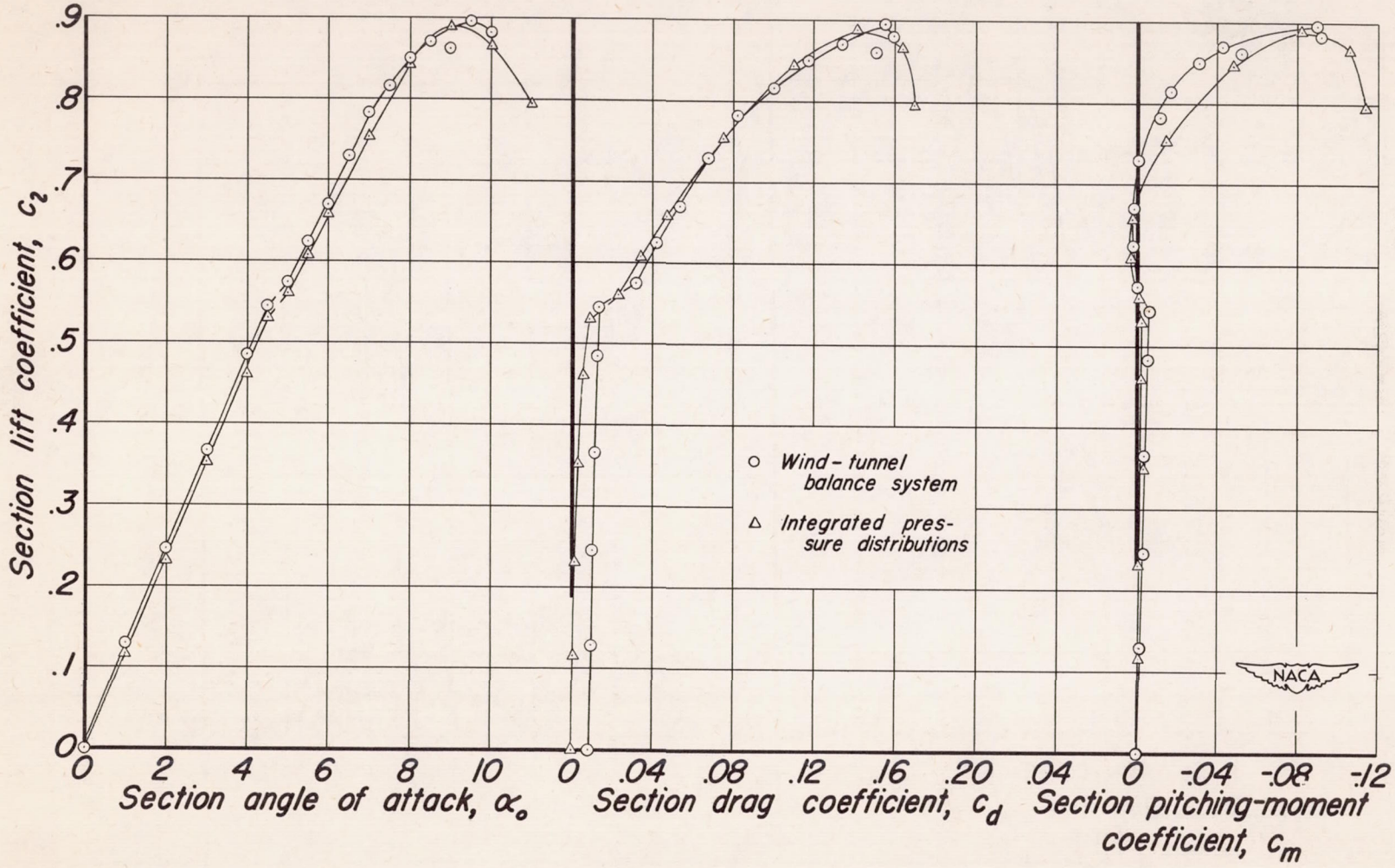

Figure 2.— Section lift, drag, and pitching-moment characteristics.

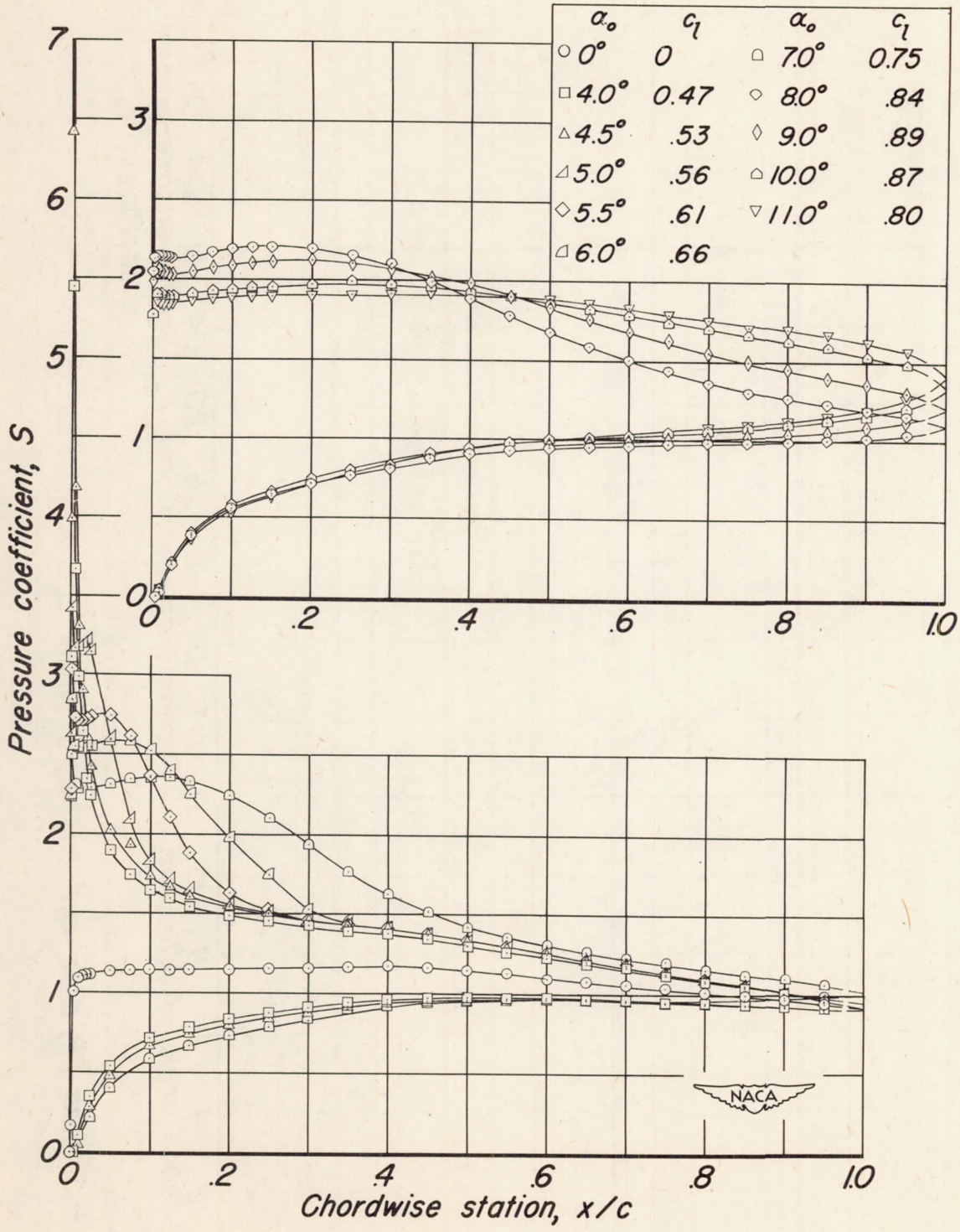

Figure 3.— Chordwise pressure distribution.

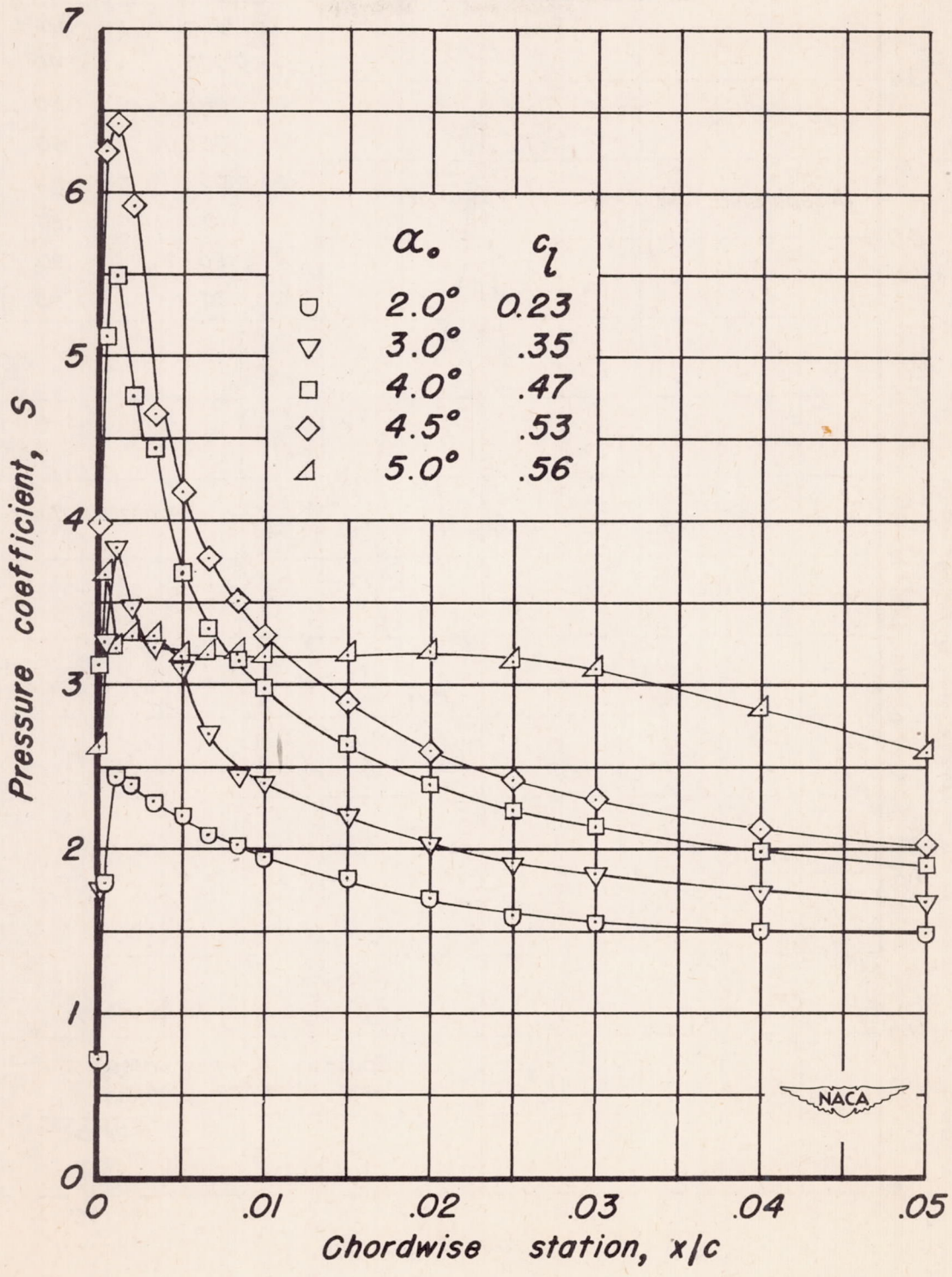

Figure 4.— Detailed pressure distribution in the vicinity of the leading edge.

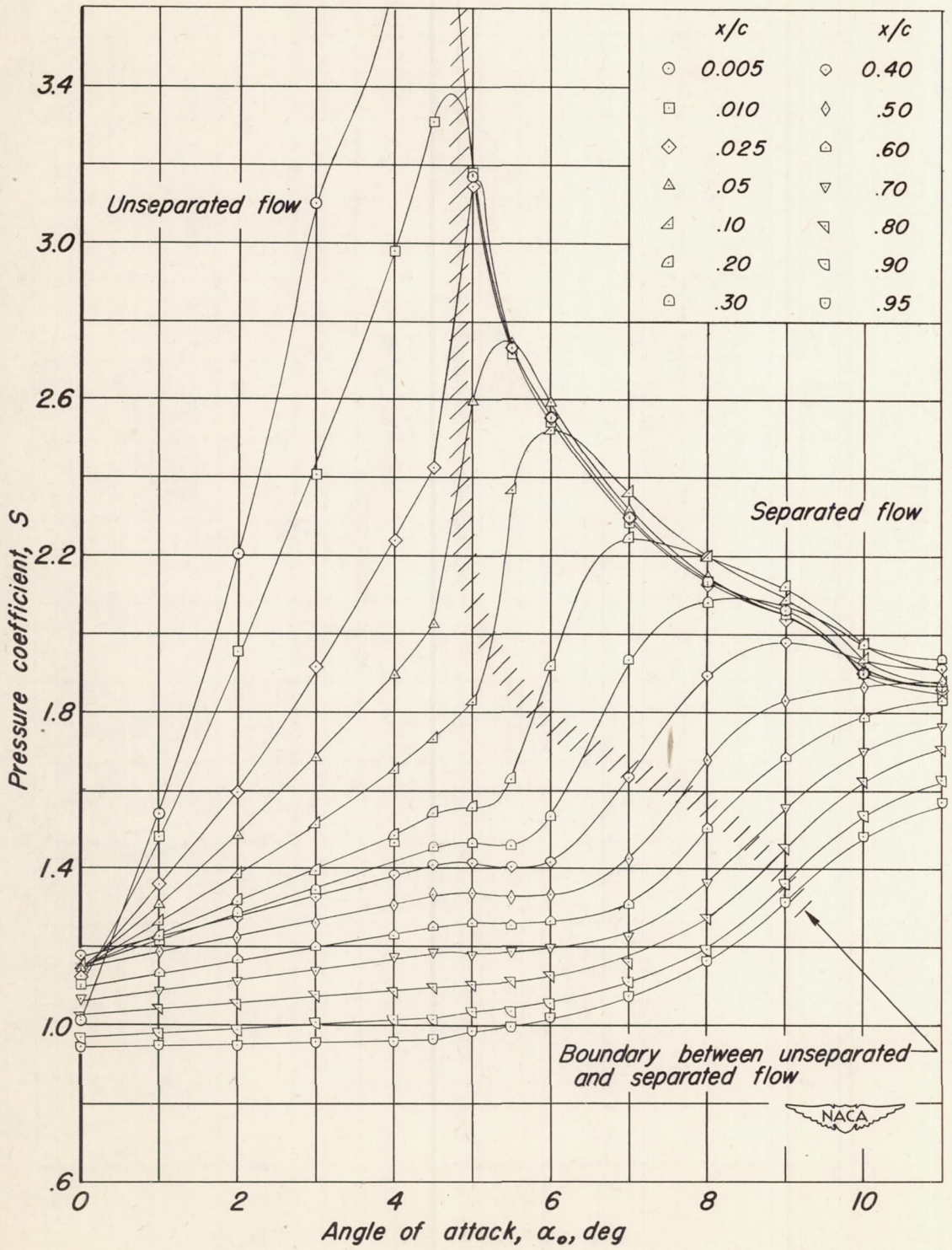

(a) Upper surface.

Figure 5.— Variation of pressure coefficient with angle of attack for various chordwise stations.

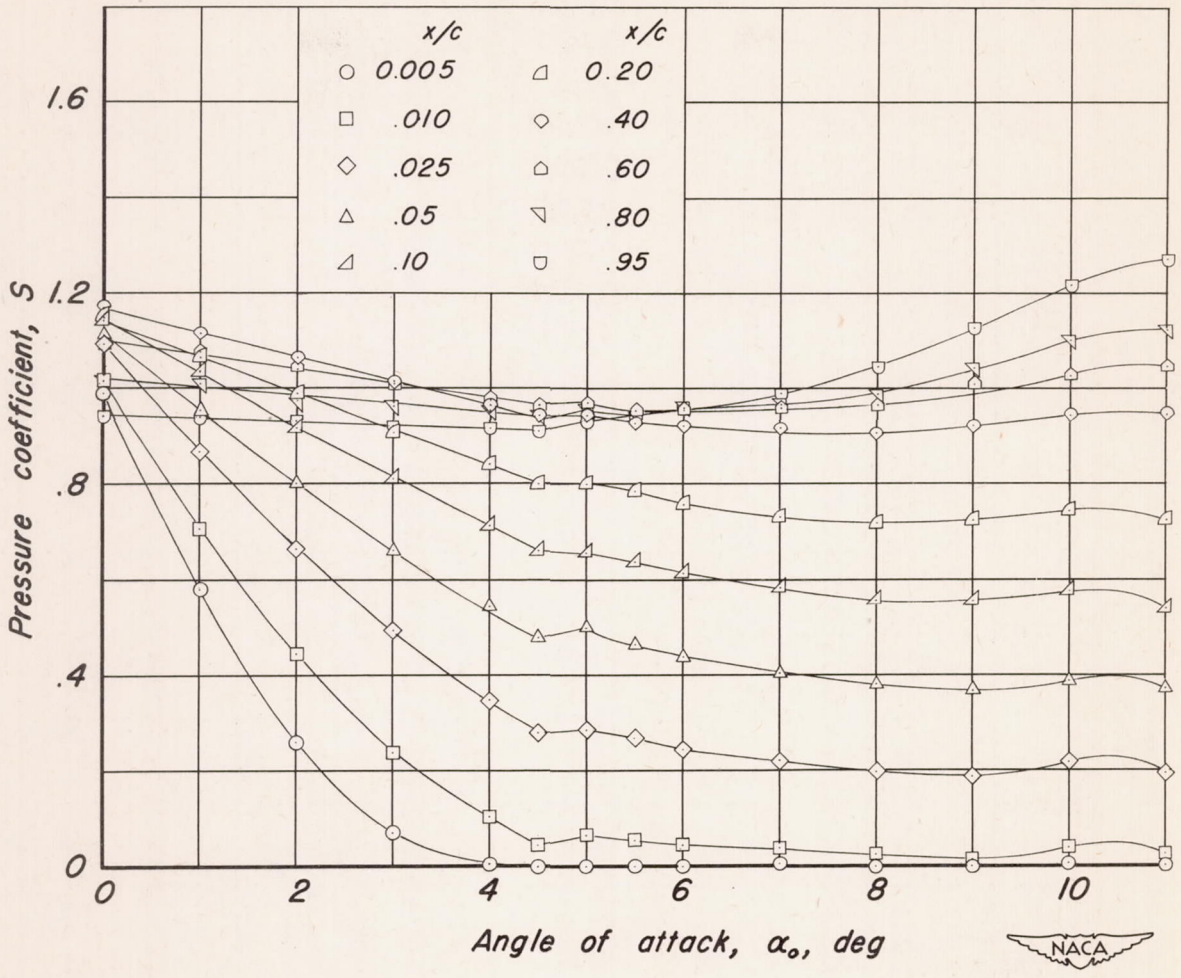

(b) Lower surface.

Figure 5.— Concluded.

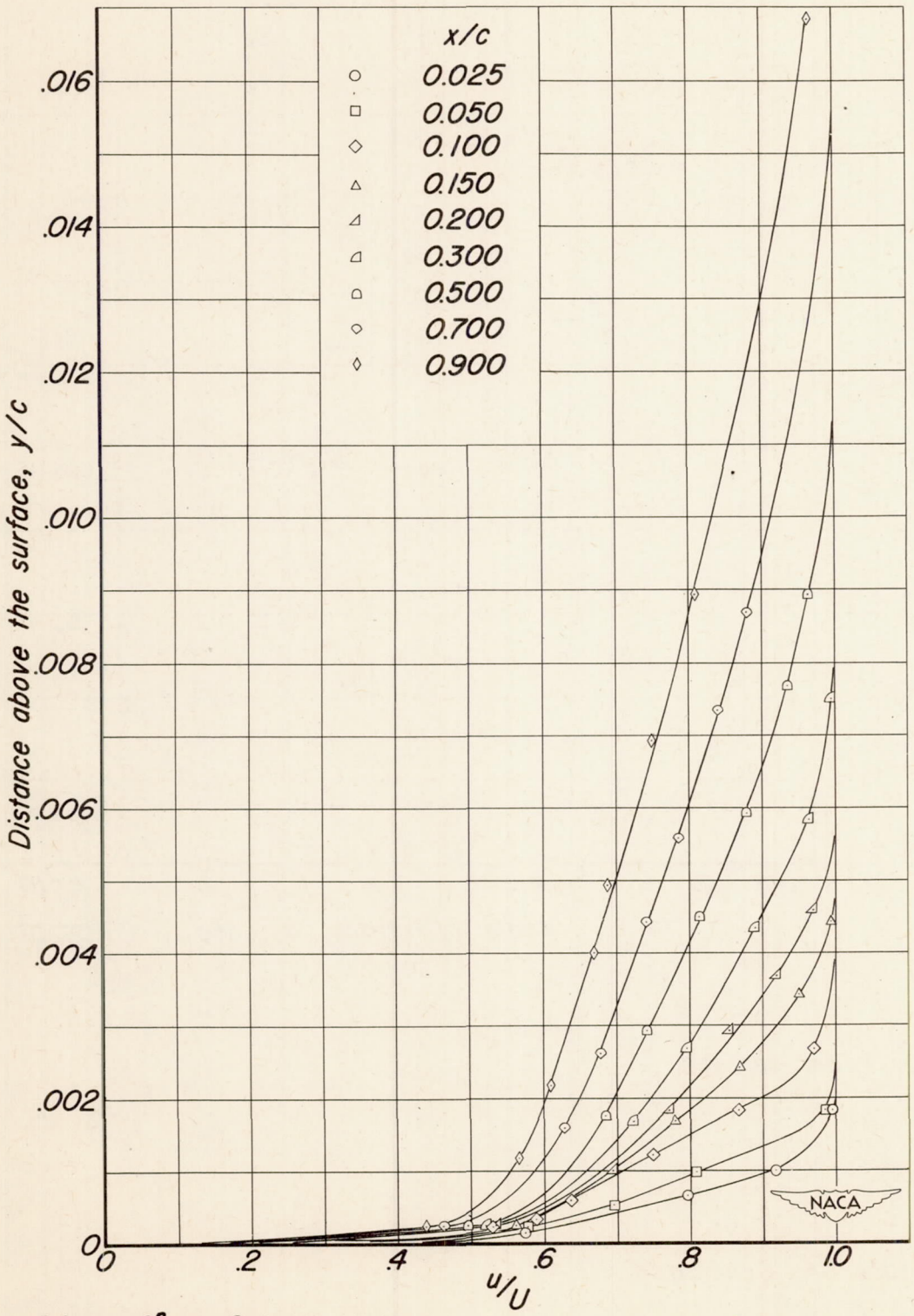

(a) α_o, 4°; c_l, 0.47.

Figure 6.—Boundary-layer velocity profiles.

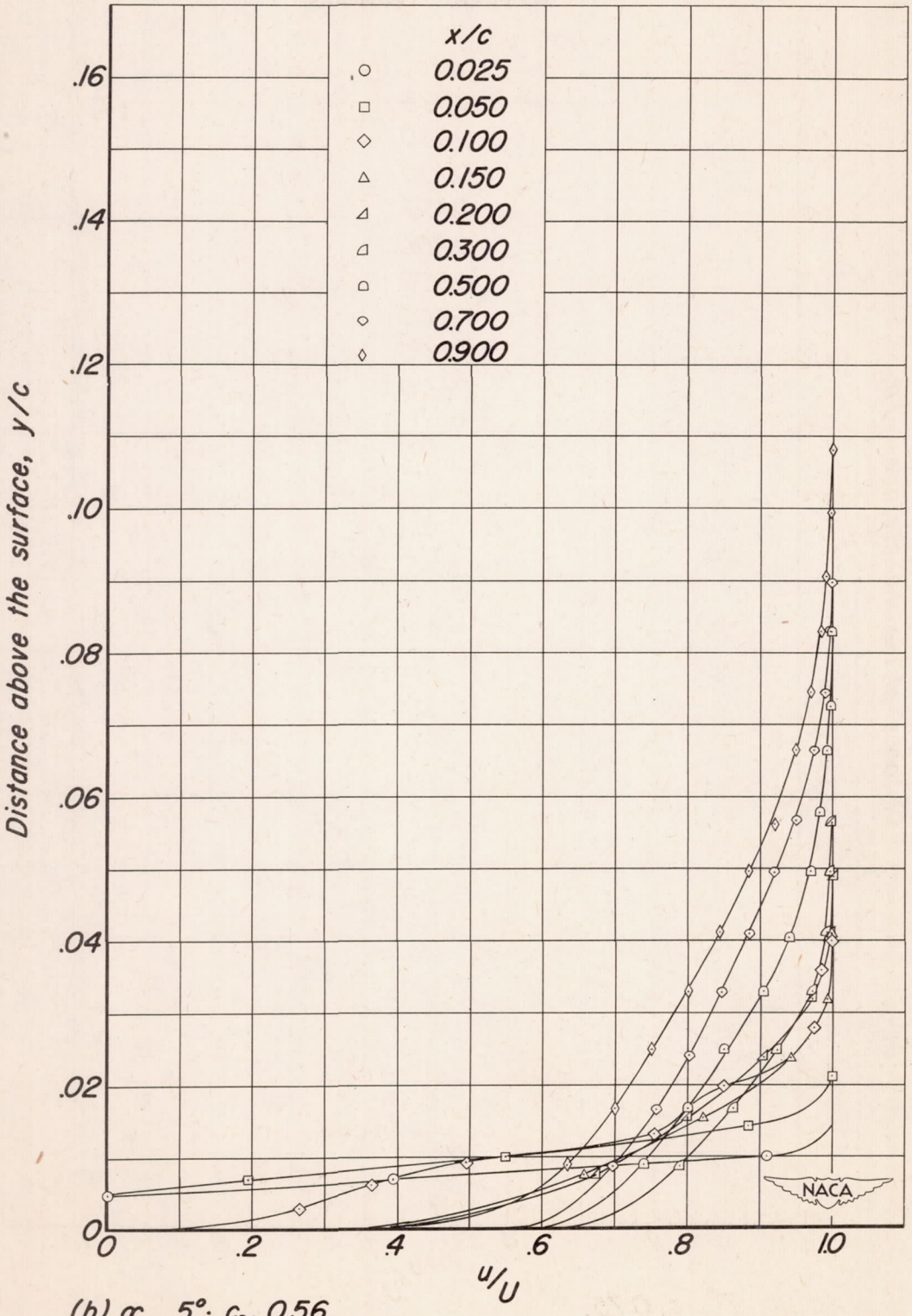

(b) α_o, 5°; c_l, 0.56.

Figure 6.– Continued.

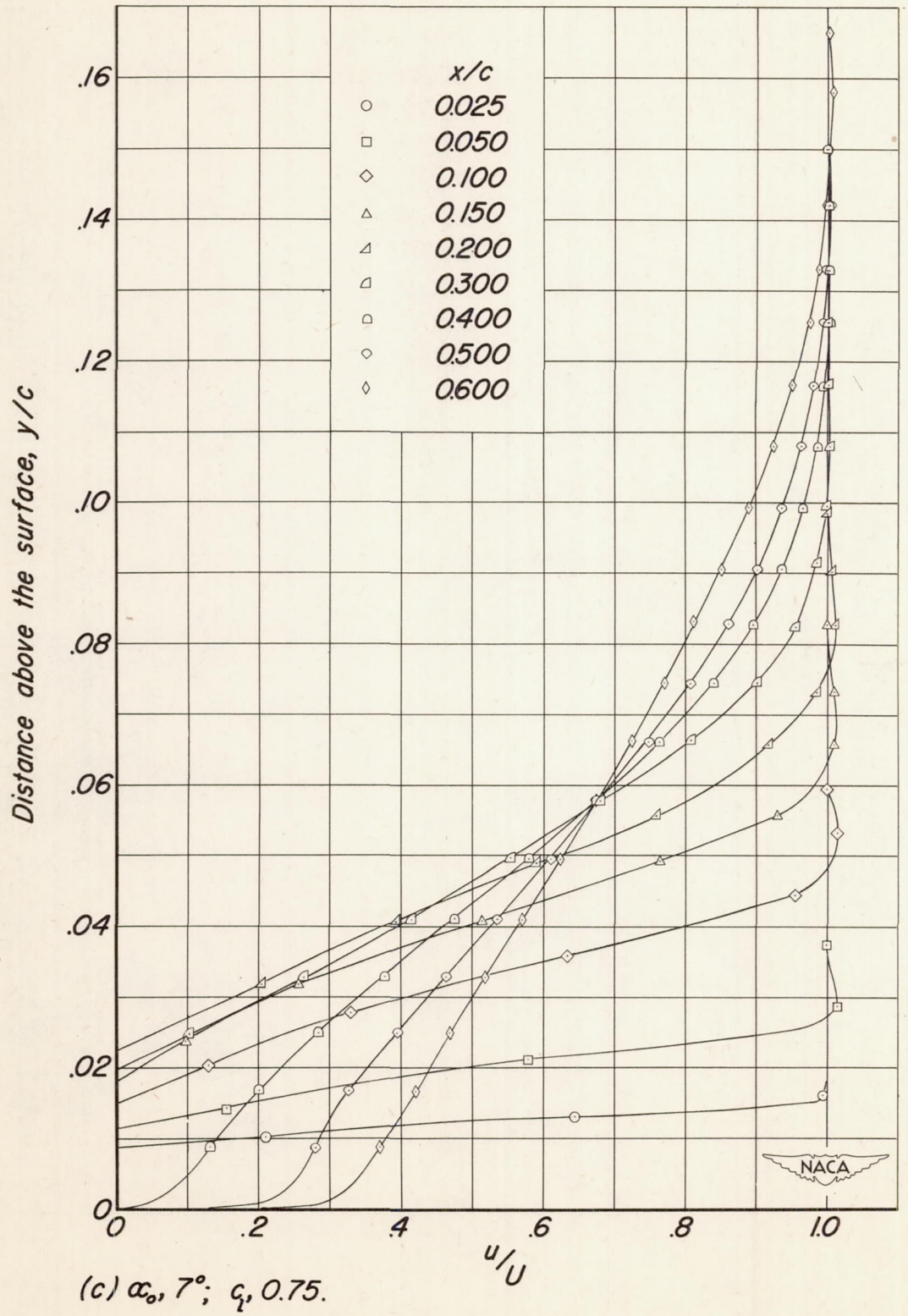

(c) α_o, 7°; c_l, 0.75.

Figure 6.— Concluded.

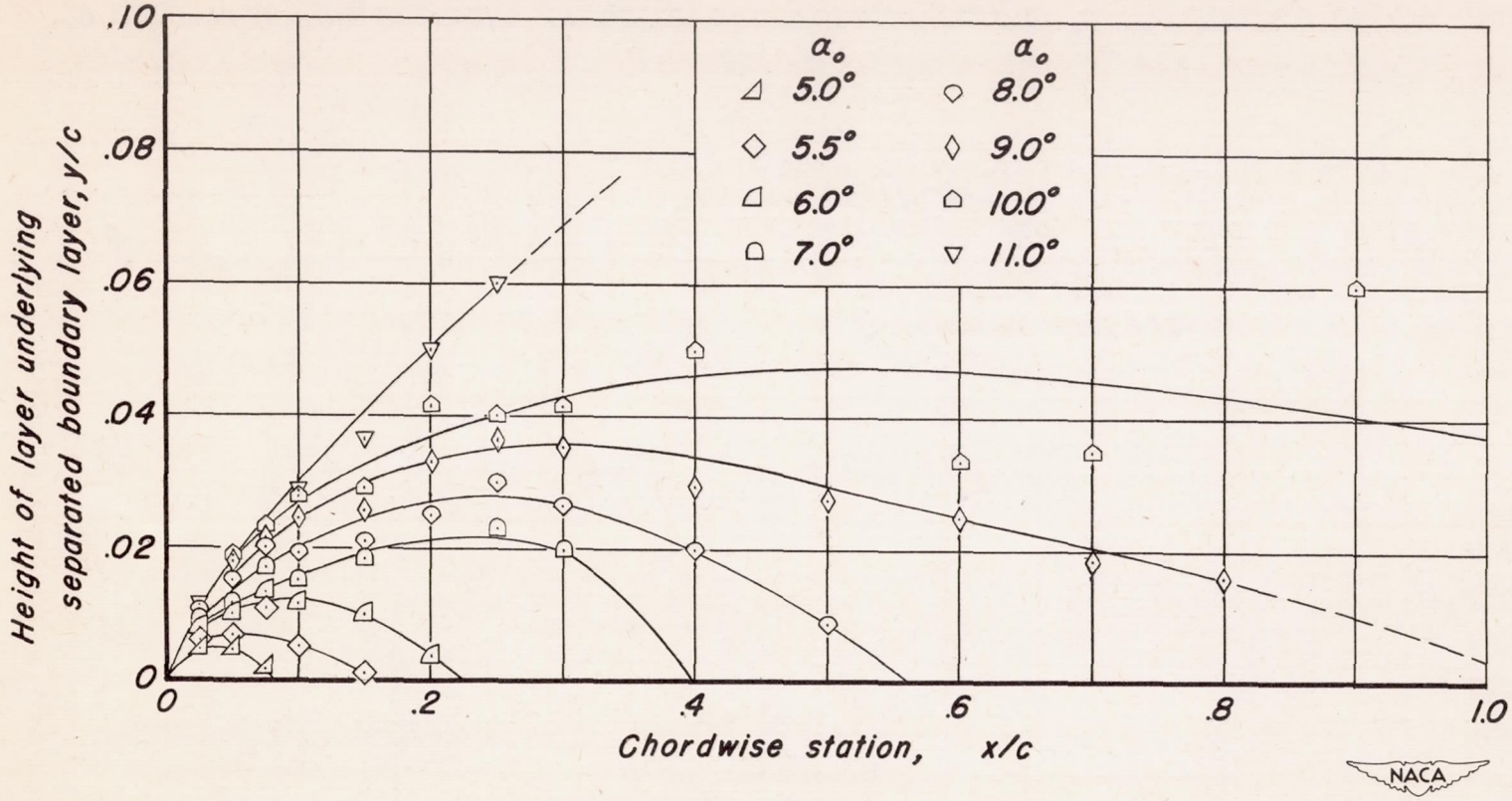

Figure 7.— Height of the layer underlying the separated boundary layer as indicated by boundary-layer surveys.

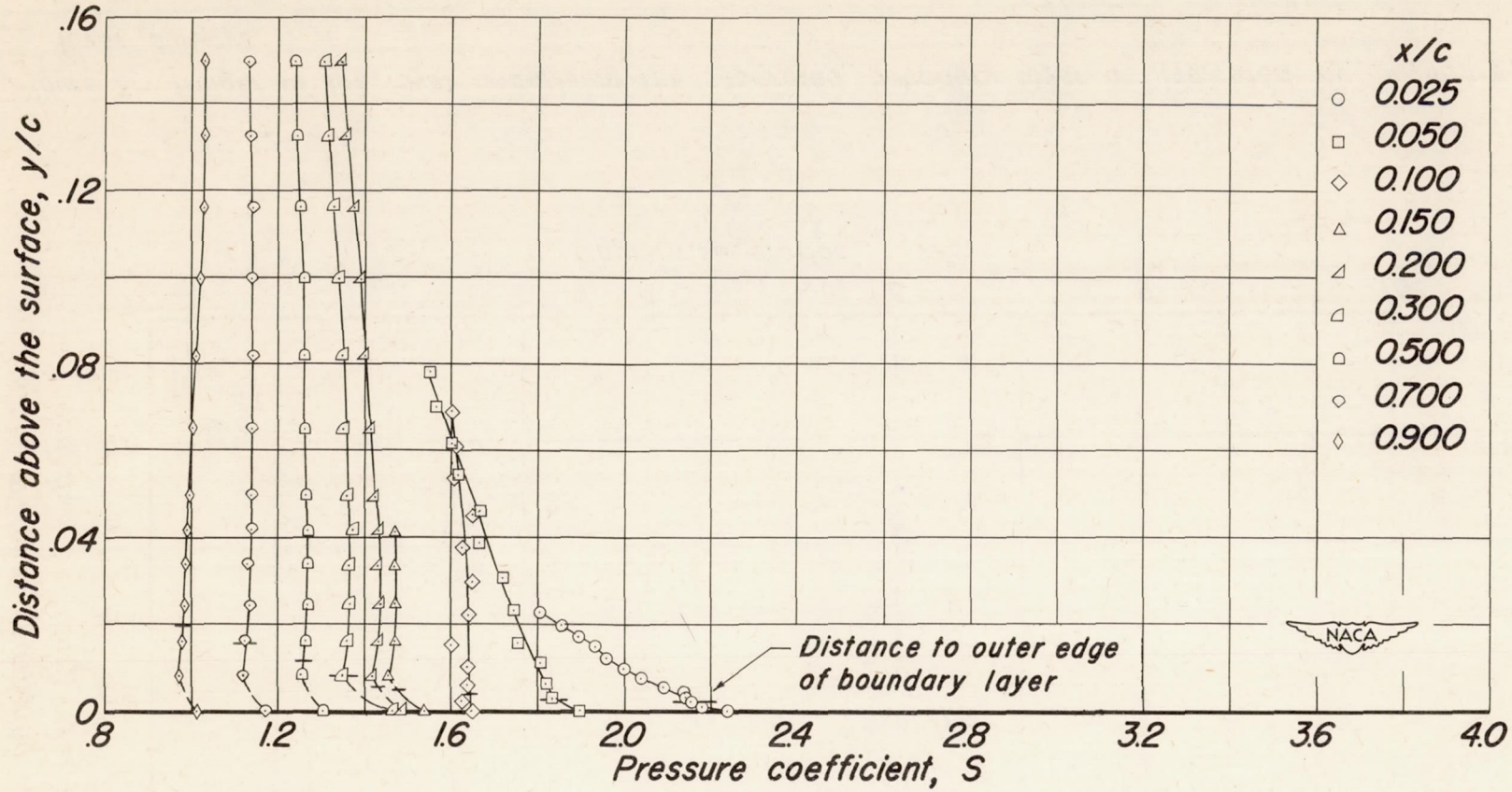

(a) α_o, 4°; c_l, 0.47.

Figure 8.—Variation of static pressure with distance normal to the surface of the model.

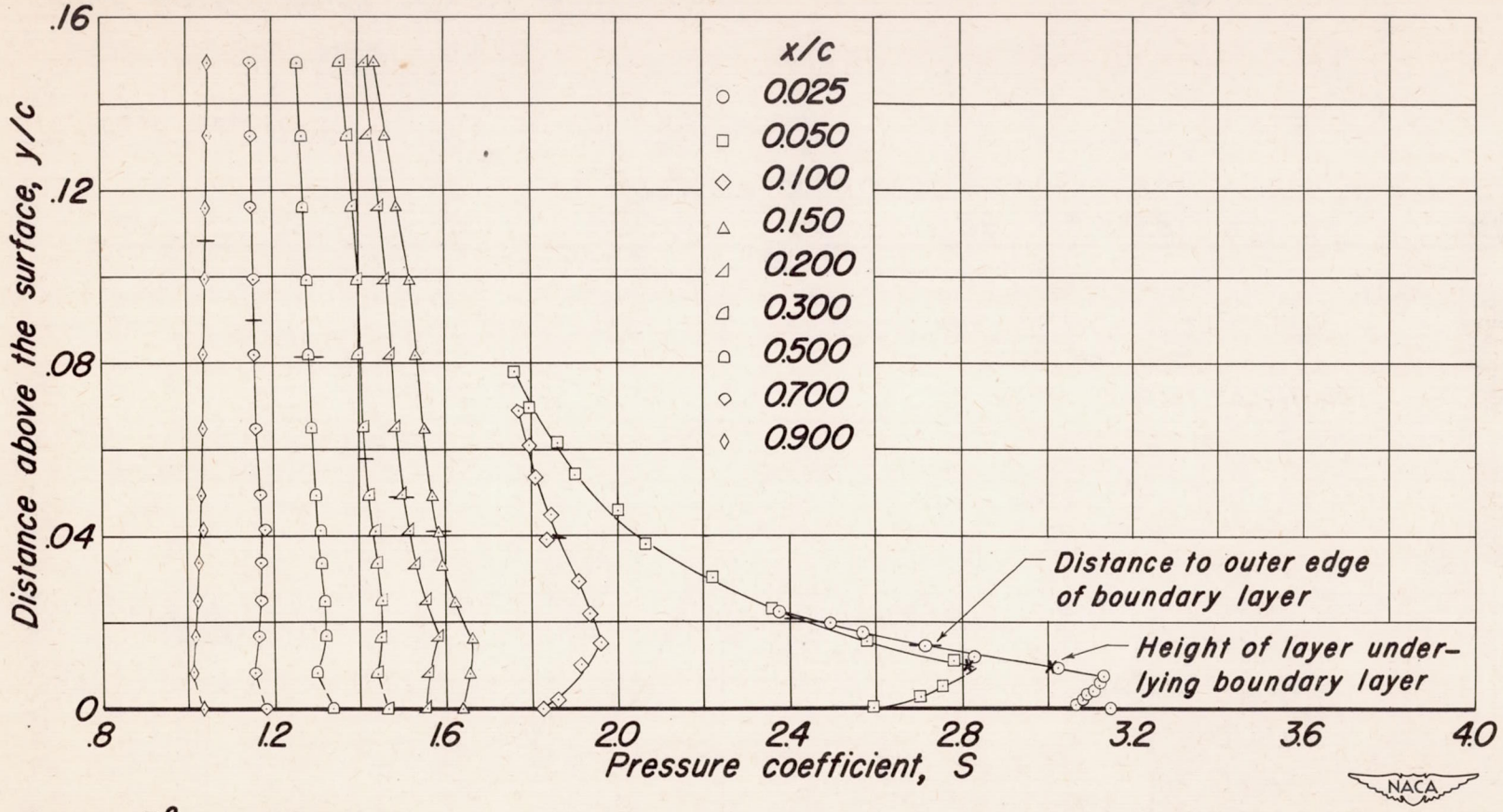

(b) α_o, 5°; c_l, 0.56.

Figure 8. – Continued.

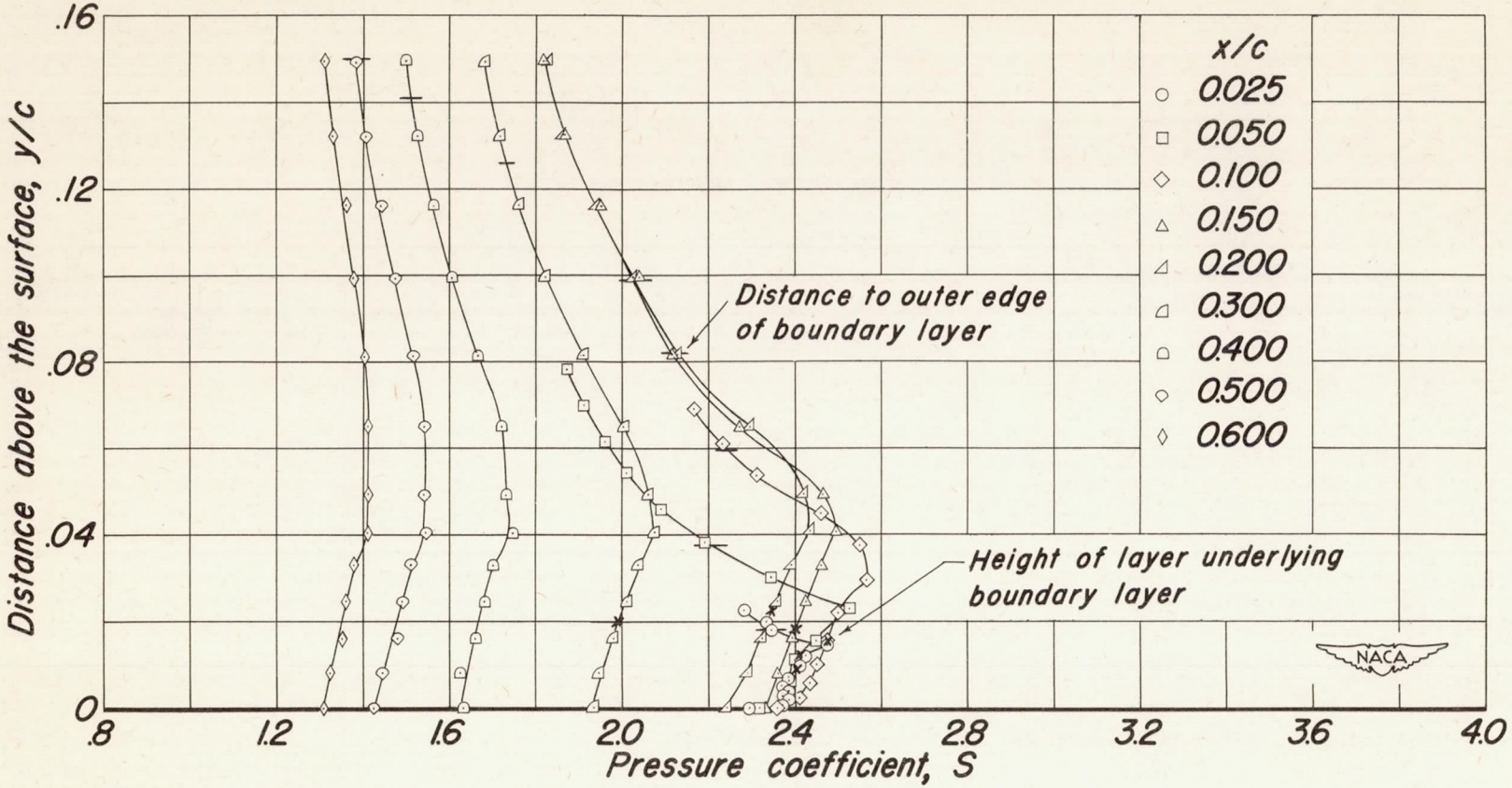

(c) α_o, 7°; c_l, 0.75.

Figure 8.— Concluded.

NACA-Langley - 8-1-49 - 1000